

LASER INTERFEROMETER GRAVITATIONAL WAVE OBSERVATORY
- LIGO -
CALIFORNIA INSTITUTE OF TECHNOLOGY
MASSACHUSETTS INSTITUTE OF TECHNOLOGY

Technical Note	LIGO-T2000290-v1	2020/11/07
Seismometer Temperature Control System		
Rushabha B		

California Institute of Technology
LIGO Project, MS 18-34
Pasadena, CA 91125
Phone (626) 395-2129
Fax (626) 304-9834
E-mail: info@ligo.caltech.edu

Massachusetts Institute of Technology
LIGO Project, Room NW22-295
Cambridge, MA 02139
Phone (617) 253-4824
Fax (617) 253-7014
E-mail: info@ligo.mit.edu

LIGO Hanford Observatory
Route 10, Mile Marker 2
Richland, WA 99352
Phone (509) 372-8106
Fax (509) 372-8137
E-mail: info@ligo.caltech.edu

LIGO Livingston Observatory
19100 LIGO Lane
Livingston, LA 70754
Phone (225) 686-3100
Fax (225) 686-7189
E-mail: info@ligo.caltech.edu

1 Introduction

The Laser Interferometric Gravitational Wave Observatory (LIGO) is designed to detect and study gravitational waves. To detect these gravitational waves, perturbations of the order $10^{-19}m$ have to be detected by the system. These changes are so small that nothing short of an engineering miracle has occurred to reduce the noise and to detect the signal in these systems. On careful study and analysis of the noise, researchers found that the lower range of the device bandwidth, lesser than $10Hz$, was dominated by seismic noise[1]. For the next generation of LIGO detectors, increasing the sensitivity and the bandwidth of the device is of the utmost importance. Hence suppression and study of seismic noise are critical to meet this goal.

The first step to understand and characterise seismic noise, is to study the motion of the ground. Sensors called as seismometers are used to detect ground motion and help us map the seismic activity in the surrounding region. These sensors need to be maintained at optimal environment conditions so that reliable readings can be obtained. Hence strict isolation from the surrounding environment and vigilant control of parameters, such as temperature is very much necessary to obtain data with the least amount of noise from the seismometers.

Multiple such sensors can be used to create a "Seismic Heat Map" of the area it is placed in. Heat maps help us better visualize the spatial distribution of the intensity of seismic activity, present in the region under study. On creating such heat maps we can use techniques of data analysis to help us identify and classify the sources of disturbance.

2 Temperature Control System

The parameters of the seismometer, most important being the temperature of the seismometer need to be strictly controlled, so that the seismic data made available to us can be further used to make reliable heat maps of the surrounding area. Such type of control can be implemented using a feedback control system, to keep the temperature of the seismometer as stable as possible. The nature of how the temperature affects the seismometer data was studied and its affect can be seen in 1. Since no temperature sensor was mounted on the seismometer to get its readings, for our analysis, we assumed that the temperature of the seismometer tracks the ambient (room) temperature, whose readings we had, with some amount of delay, which was later compensated in python.

In 1, the effect of the temperature gradient(foreground) on the seismic noise (background) can be clearly seen in the upper plot i.e. the lower frequency range when compared to the bottom plot i.e. the higher frequency range. We can see that there is a positive correlation between the temperature gradient and the noise floor in the seismometer. To confirm this the pearson nr correlation metric was used to get the dependence of the temperature gradient and the noise spectrum across the frequency range of interest, which can be seen in 2. The figure contains the correlation of the noise with the temperature gradient in all the three data streams i.e. X,Y and Z of one of the seismometers present in the lab. From the figure we can see that there is a much higher correlation of the temperature gradient on the seismic noise at lower frequencies when compared to the higher ones, confirmed visually by

1 as well.

Hence from this we can understand that if we can control the temperature, essentially making the gradient tend to zero then we can prevent this fluctuation of seismic noise present in our data.

To accomplish this, the seismometer under study is mathematically modelled and simulated in the time as well as in the frequency domain. Linear PID controller has been implemented, so that the temperature of the seismometer tracks the reference temperature with the least amount of error and with reasonable amount of latency.

The feedback control system to be designed to control the temperature of the seismometer is as shown in 3

3 Modelling of the control system

3.0.1 Modelling of the seismometer apparatus

Modelling of the system is done based on the physical setup in the lab. The setup can be visualized crudely by seeing 4

The seismometer heating apparatus can be mathematically modelled using the heat equation as :

$$P_{in} = M_{ss}C_{ss} \frac{dT_{ss}}{dt} + P_{loss} \quad (1)$$

The loss for this model is assumed to be purely conductive in nature, due to the presence of the foam wrapping between the environment and the stainless steel box which makes the radiative losses negligible when compared to the conductive losses.

$$P_{loss} = \frac{k_{foam}A_{foam}}{t_{foam}}(T_{ss} - T_{amb}) \quad (2)$$

Considering the mentioned assumptions, we get the relation between the input heating power and the temperature of the stainless steel box, in the laplace domain as:

$$T_{ss}(s) = \frac{P_{in}(s) + B}{M_{ss}C_{ss}s + A} \quad (3)$$

$$B = k_{foam}A_{foam}t_{foam}T_{amb} \quad A = k_{foam}A_{foam}t_{foam}$$

Refer to Appendix A for complete derivation of the mathematical model.

Hence the natural response of the system with $P_{in}(s)$ equated to zero gives us the plant transfer function, which is completely dependent on the ambient temperature response :

$$T_{ss}(s) = \frac{R_f}{L_{ss} * s + R_f} * T_{amb}(s) \quad (4)$$

$$R_f = A/t_{foam} \quad L_{ss} = M_{ss} * C_{ss}$$

Where R_f is the thermal resistance of the foam covering and L_{ss} is the natural thermal inductance of the system.

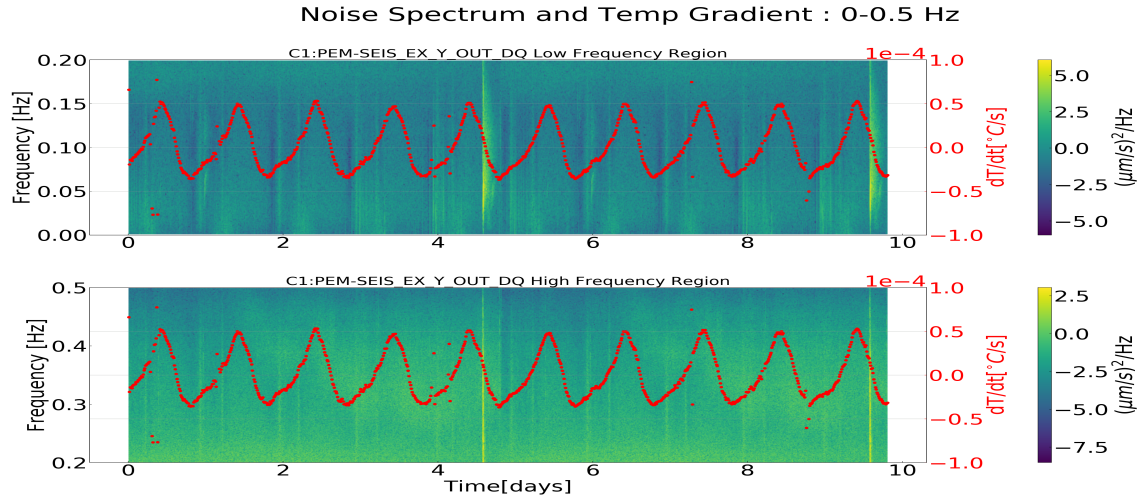


Figure 1: Temperature gradient and Noise spectrum

Pearson Correlation wrt dTempdt : 0.01-0.1 Hz

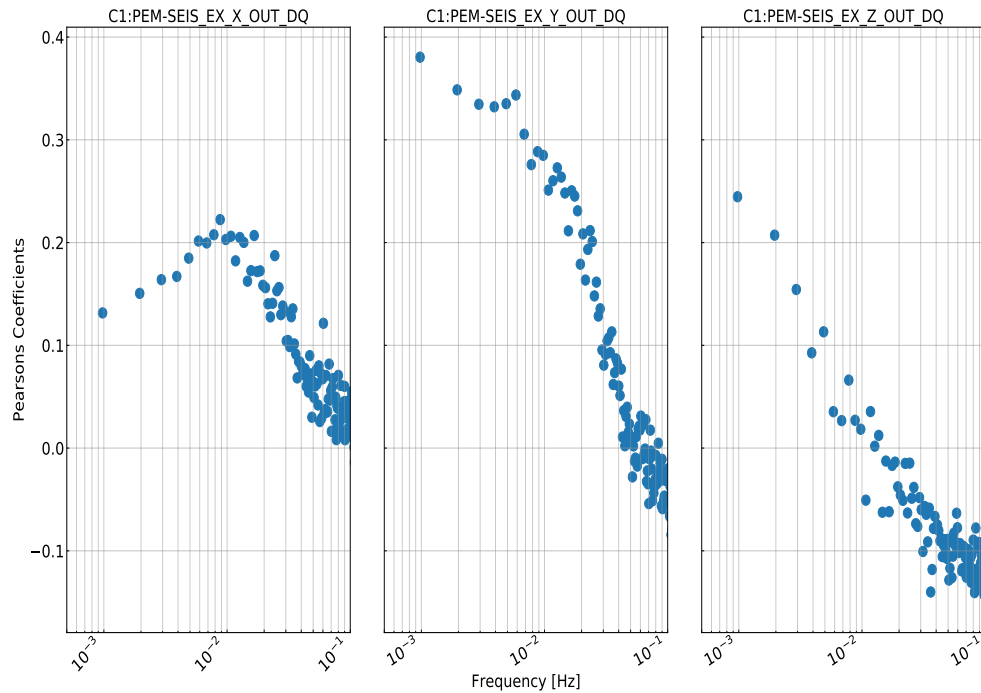


Figure 2: Temperature gradient and Noise spectrum Correlation

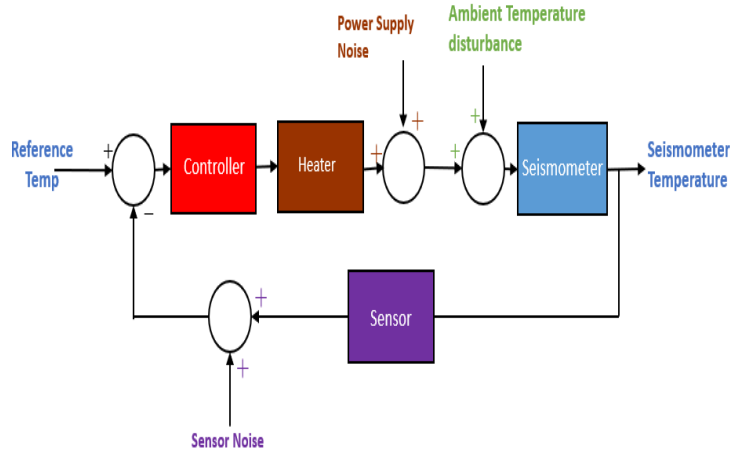


Figure 3: Temperature Control System

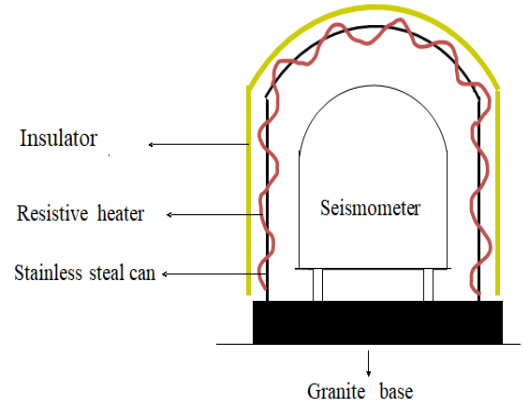


Figure 4: Physical setup of seismometer

3.1 Modelling of the Ambient Temperature fluctuation

The ambient temperature data was obtained from the nds2 client from the sensors present in the LIGO lab, which monitor the room temperature. Since the ambient temperature acts as a main source of disturbance for the 'set point' of the temperature of the seismometer, modelling its effect on our system is very important.

Data for a period of 30 days was downloaded using the nds2 client. The time series data for the 30 day period is shown in 5. For finding the power spectrum the pwelch algorithm was used. Since the frequency of the variation in the data is in days, an appropriate large window had to be chosen so that the welch algorithm could identify the correct lower frequency range. The daily fluctuation i.e. the 24 hour cycle of heating and cooling had to be present as a peak approximately at $1.153 \times 10^{-5} Hz$ in the power spectrum. Keeping this as a marker the *nperseg* parameter of the *pwelch* function was changed until one could see this peak. For a sampling frequency of $1/60 Hz$ the *nperseg* was chosen to be $1024 * 8$. The power spectrum of the ambient temperature data is shown here 6

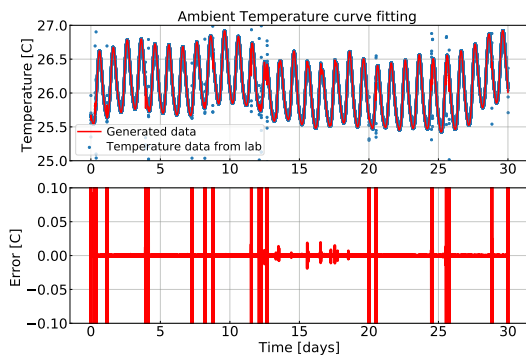


Figure 5: Time series data of Ambient Temperature

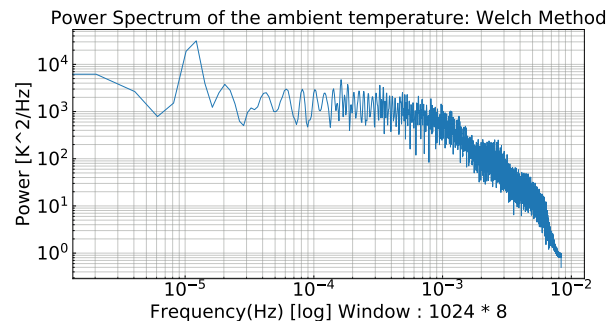


Figure 6: Power Spectrum of the Ambient Temperature

Since the data was noisy and glitches were present very frequently, a curve fitting algorithm was developed so that we could develop a function preventing the need to download the data.

It also helped us clean out the glitches present in the data. A cubic spline interpolation was chosen to be the best method to fit the data, in this method cubic curves are simulated to fit different pieces of the data. The results are very ideal, as can be seen in 5. The curve fit generated data is shown in red.

The only disadvantage with this method is that the function can provide data only for the duration it was created with, for our case data for 30 days was used, we cannot use this function to generate data for more than this period. Hence a large duration was chosen to create the interpolation function so that we can run the simulations with some reasonable accuracy.

3.2 Modelling the different noise sources

The two major sources of noise that are present in our system are :

- Power Supply Noise : The noise was assumed to be gaussian with zero mean and whose variance was calculated from known RMS power of the noise . However the implementation into the control loop was not direct. The total power for the system was calculated using the differential power in the ODEint solver, hence for the known power supply noise variation this could not be directly introduced as an additive quantity. An approximation of the noise power i.e. its variance had to be made by looking at the output power fluctuation and seeing if it matched the variation which we had anticipated originally.
- Sensor Noise : The noise for this source was also assumed to be gaussian with zero mean and some variance. This variance was determined by referring to [5], where extensive study of the noise from thermistors have been made and the RMS power fluctuation of the sensor noise is stated for the most popular temperature sensors currently being used in the market.

3.2.1 Noise Budget of our System

The Amplitude Spectrum Density (ASD) of both the noise sources and the ambient temperature fluctuation is calculated and is put in one plot for easy visulation of the total noise present in our system 7. To generate 7 the square root of the power spectral density (PSD) was taken and the PSD was obtained for each source using the *pwelch* function with a sampling frequency of 1/10 Hz and *nperseg* of 1024 * 48.

3.3 Design of controller

The controller chosen was the Proportional-Integral-Derivative(PID) controller.The parameters to be tuned for such a controller and their effect on the system is explained below:

1. K_P : The proportional constant, this parameter helps to move the closed loop poles along the root locus, to get the best transient response.

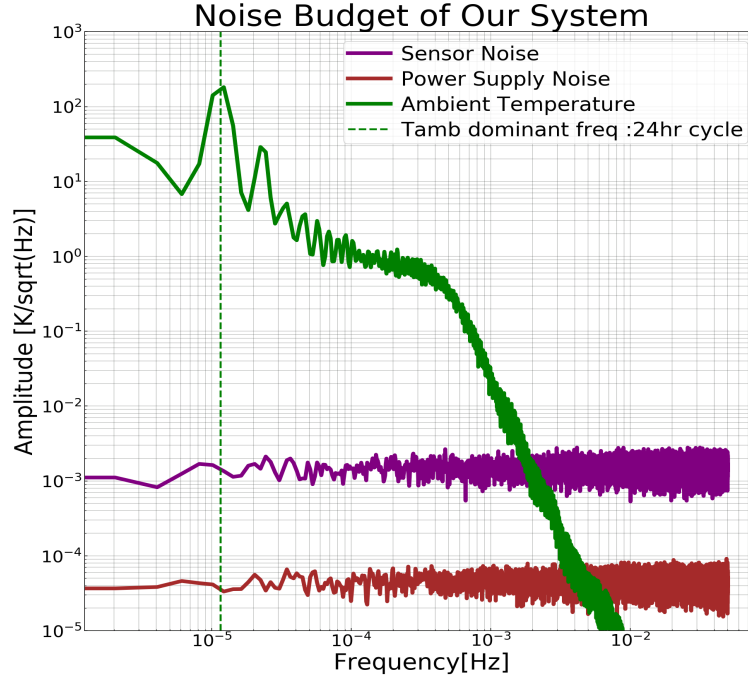


Figure 7: Amplitude Spectrum Density of the system noise and disturbances

2. K_I : The integral constant is varied to reduce the steady state error of the output signal.
3. K_D : The derivative constant is tuned to get the best transient response, when the desired values that is expected of the output response are outside the root locus.

Combining all the above constants, the PID block in the laplace domain is defined as:

$$H_1(s) = K_P + \frac{K_I}{s} + sK_D \quad (5)$$

The same thing in the time domain can be represented as:

$$e_{PID}(t) = K_P e(t) + K_I \int_0^t e(\tau) d\tau + K_D \frac{de(t)}{dt} \quad (6)$$

where $e(t)$ is the error signal that is passed through the PID block and then e_{PID} is fed into the PWM circuit.

To determine the values for the PID parameters a cost function which encapsulates the necessary objectives to minimise is used.

3.3.1 Formulation of Cost Function

The error temperature, given as :

$$T_{err}(t) = T_{ss}(t) - T_{ref} \quad (7)$$

where T_{ss} is the seismometer temperature and the T_{ref} is the reference temperature. The T_{err} is analysed in the time and frequency domain only for the steady state condition i.e. for time greater than t_s , where t_s is the settling time of the system. The settling time defined for this system is the time it takes for the output temperature to come within the 5% range of the reference temperature when the system is subjected to a step response.

With the unoptimised PID coefficients i.e. using manual tuning the steady state error in the time and frequency domain 8 was analysed. Anaysis carried out in the frequency domain gives us a better insight into what our error consists of, here we can see that the peak near $10^{-5}Hz$ is the same peak we see in the ambient temperature power spectrum, telling us that the ambient temperature fluctuation has a higher impact on the output temperature when compared to the sensor and power supply noise.

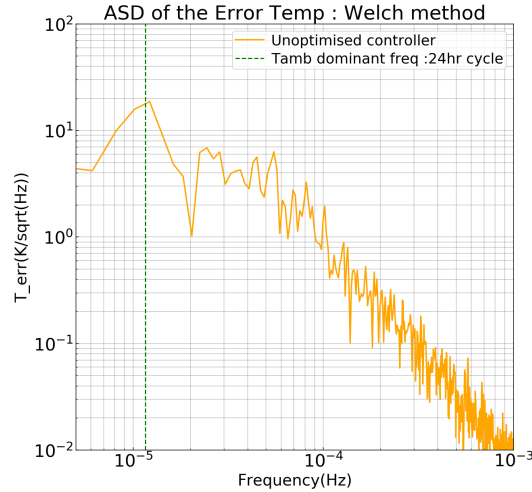


Figure 8: Steady state error in the frequency domain

Hence the cost function in the frequency domain was considered to be the total fluctuation caused due to T_{amb} , power supply noise PS_n and the sensor noise S_n at the output i.e. the seismometer temperature. In the frequency domain we can formulate this as the following :

$$\Delta T_{ss}^2(f) = [\Delta T_{amb}(f) * Y_1(f)]^2 + [\Delta PS_n(f) * Y_2(f)]^2 + [\Delta S_n(f) * Y_3(f)]^2 \quad (8)$$

$$CostFunction = \int_{f1}^{f2} \Delta T_{ss}^2(f) df \quad (9)$$

where $Y_1(f)$, $Y_2(f)$ and $Y_3(f)$ are the closed transfer function of T_{ss} to the respective disturbances and noise. The integral of this disturbances across the frequency range i.e. $0 - 1Hz$ will be minimised. The transfer functions are carefully calculated from each injection node of the noise/disturbance in the control system block diagram 9 to the output node.

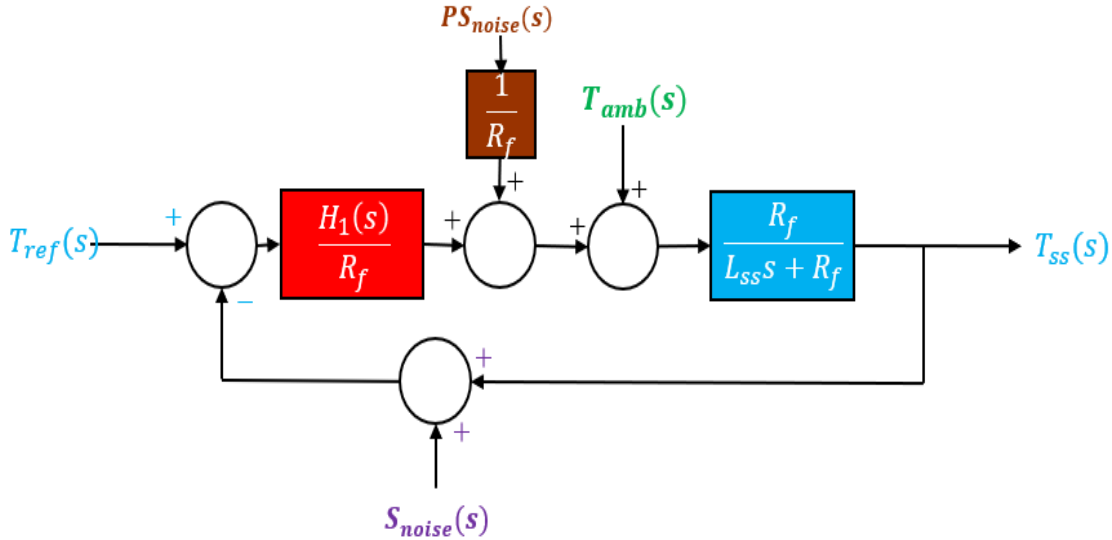


Figure 9: Frequency domain model of the complete system

To find the PID coefficients which minimised this cost function the Particle Swarm Optimization (PSO) algorithm was used.

4 Results

4.1 Transfer Function

The bode plots for the transfer function, obtained from the optimised PID controller, for the dominant disturbance i.e. the ambient temperature is shown in 10.

The loop gain of the system is analysed to see if the system is stable and to check for the unity gain bandwidth (UGB) 11. As you can see from the plot, the system is stable at UGB due to the presence of almost 75° of phase margin.

4.2 Steady State Error and Noise budget at output

The frequency domain of the steady state error for the optimised and the unoptimised PID parameters is shown in the figure 12 with the suppression of the dominant noise frequency highlighted in green. Hence with the correct PID coefficients we can ensure that the impact of disturbances at the seismometer temperature output is as low as possible. However it should be noted that the minimum level of noise at the output that we can achieve using our controller will always be limited by the sensor noise.

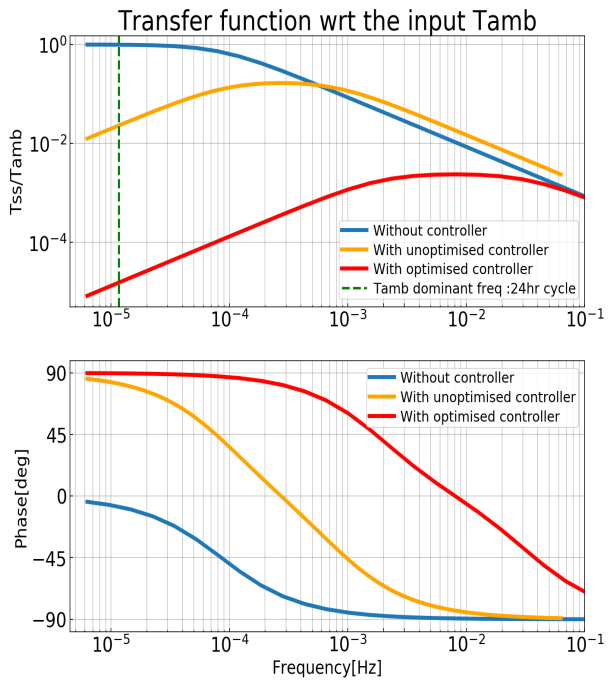


Figure 10: Ambient Temperature transfer functions

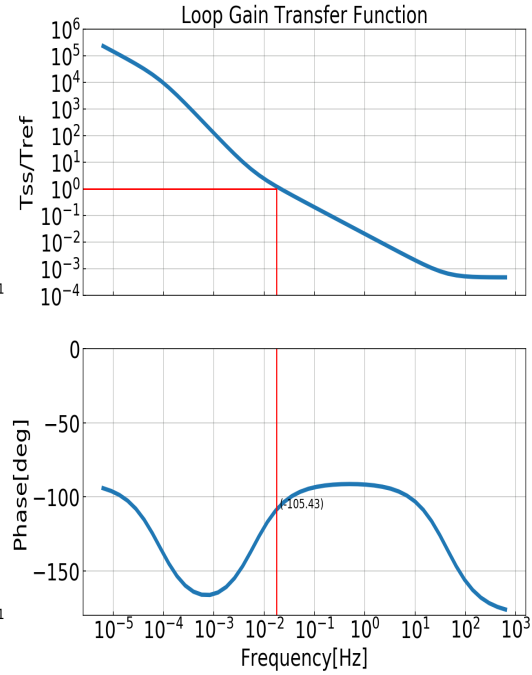


Figure 11: Loop gain of the system

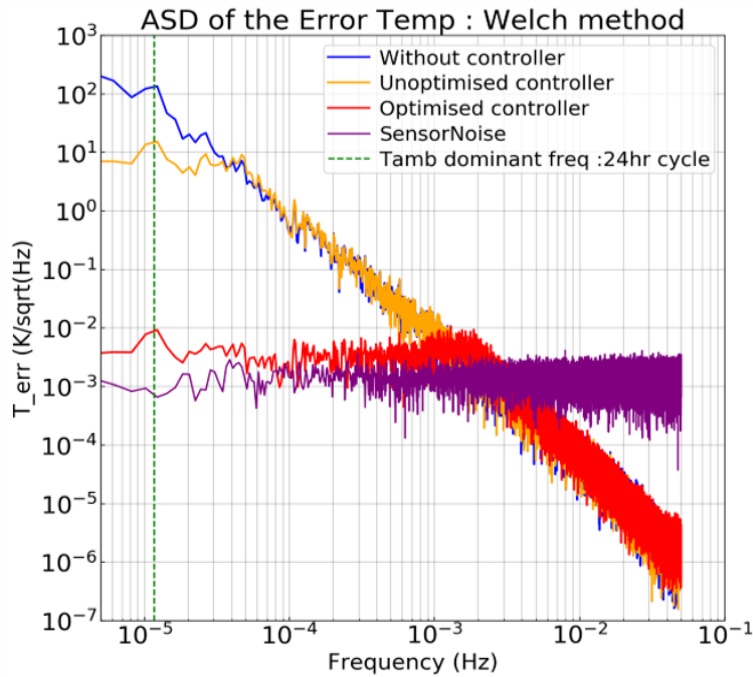


Figure 12: Comparison of the steady state error

5 Conclusions

I have been able to simulate the seismometer setup in the lab and the impact of the different noise sources on it. Implement a linear PID controller to control the temperature of the simulated plant and optimise this PID controller using the Particle Swarm Optimisation (PSO) algorithm on the defined cost function.

The hardware design of a remote heater setup has also been done but however I was not successful in completing the hardware implementation of the system.

6 Future Work

The future work for this project would be :

- Implement the simulated system on hardware especially in the LIGO lab or a similar such environment.
- Using a more robust cost function and compare the results of the new PID coefficients with the ones I have used.
- Implement a non-linear feedback controller i.e. a neural network controller on the hardware implementation and compare it with the linear PID controller.

7 Acknowledgments

I would like to thank my mentors Prof.Rana Adhikari, Dr.Koji Arai and Dr.Tega Edo for all their guidance and support throughout the project. I would also like to thank my SURF teammates for helping me and making the internship experience an enriching one.

Finally I would like to thank the LIGO community, National Science Foundation (NSF) and LIGO-India for providing me this opportunity to help me grow my research potential.

A Derivation of the mathematical model for seismometer heat apparatus

The seismometer heating apparatus was mathematically modelled using the heat equation :

$$P_{in} = M_{ss}C_{ss} \frac{dT_{ss}}{dt} + P_{loss} \quad (10)$$

The loss for this model is assumed to be purely conductive in nature, due to the presence of the foam wrapping between the environment and the stainless steel box.

$$P_{loss} = \frac{k_{foam}A_{foam}}{t_{foam}}(T_{ss} - T_{amb}) \quad (11)$$

Substituting (10) in (9) and integrating (9), we get:

$$T_{ss}(t) = \frac{1}{M_{ss}C_{ss}} \left[\int_0^t P_{in}(\tau) d\tau - \int_0^t \frac{k_{foam}A_{foam}}{t_{foam}} (T_{ss}(\tau) - T_{amb}) d\tau \right] \quad (12)$$

Rearranging the terms we have :

$$T_{ss}(t) + \frac{1}{M_{ss}C_{ss}} \int_0^t \frac{k_{foam}A_{foam}}{t_{foam}} T_{ss}(\tau) d\tau = \frac{1}{M_{ss}C_{ss}} \left[\int_0^t P_{in}(\tau) d\tau + \frac{k_{foam}A_{foam}}{t_{foam}} T_{amb} t \right] \quad (13)$$

Differentiating (12):

$$\dot{T}_{ss}(t) + \frac{1}{M_{ss}C_{ss}} \frac{k_{foam}A_{foam}}{t_{foam}} T_{ss}(t) = \frac{1}{M_{ss}C_{ss}} P_{in}(t) + \frac{1}{M_{ss}C_{ss}} \frac{k_{foam}A_{foam}}{t_{foam}} T_{amb} \quad (14)$$

Converting the time domain equation to laplace domain:

$$T_{ss}(s) = \frac{P_{in}(s) + B}{M_{ss}C_{ss}s + A} \quad (15)$$

$$B = \frac{k_{foam}A_{foam}}{t_{foam}} T_{amb} \quad A = \frac{k_{foam}A_{foam}}{t_{foam}}$$

B Remote Heater Model

A remote heater toy model of the seismometer setup was also designed, by ordering the necessary components online. The seismometer (plant) was replaced with a cup and the entire control system was governed by a raspberry pi microcontroller. The aim of this system was to keep the temperature of the cup as stable as possible. The system schematic is shown in [13](#)

The main components chosen and the reason behind choosing them is outlined below :

- Raspberry pi : Powerful microcontroller which can run python scripts and has large number of useful peripherals including Pulse Width Modulation(PWM).
- MOSFET: The switching device to our heater was chosen to be a MOSFET, since it is a voltage controlled device integrating it with a microcontroller would become very easy. Since this entire setup was being done on a breadboard , low voltage and low power switching MOSFET was chosen. Hence the logic level MOSFET, IRL540NbF, which turned on completely at 3.3V was chosen to be our switch.
- Pulse Width Modulation (PWM) : PWM was chosen as the means of control for the MOSFET as it allows the MOSFET to be in one of two possible states i.e. 'ON' or 'OFF'. This prevents the MOSFET entering an interim state of high resistance which leads to large amount of power loss. This causes the MOSFET to heat up which may lead to the damage of the device. Hence PWM modulation is used to convert the output of the PID controller present in the raspi, as code, into a duty cycle which controls the MOSFET.

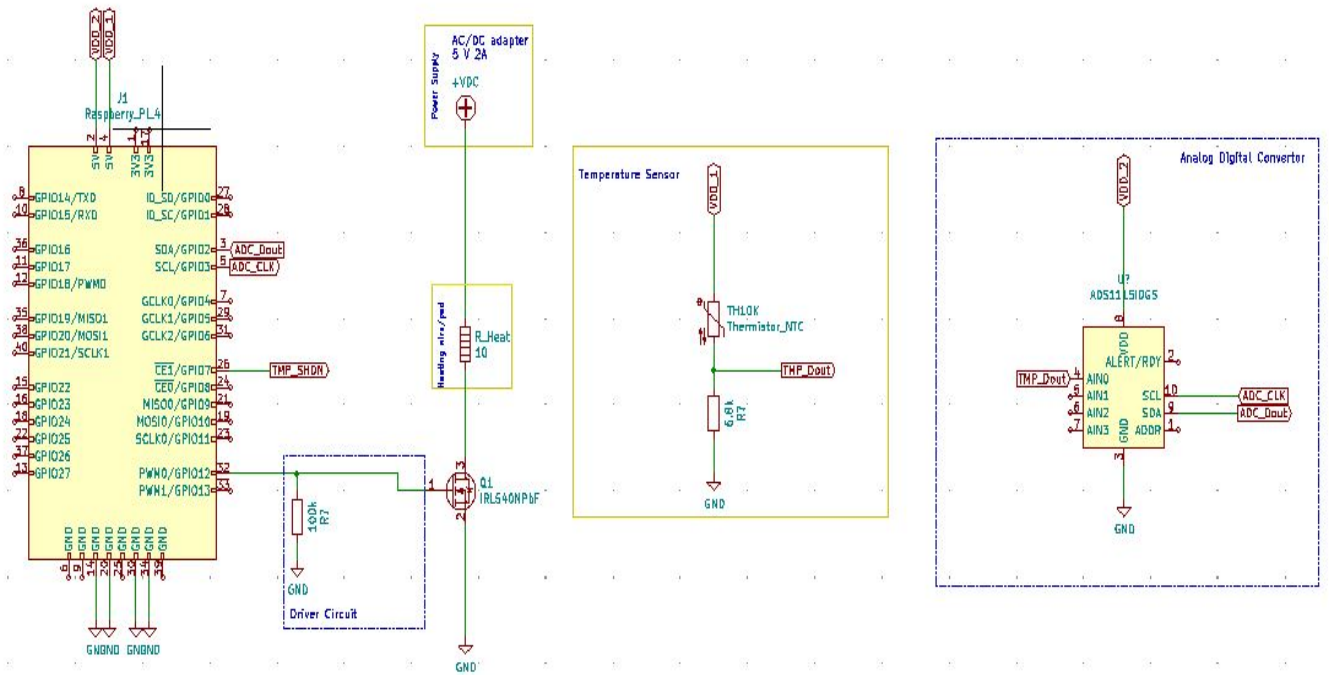


Figure 13: Remote System model : Detailed schematic

- Temperature sensors : Thermistors, or resistors whose value is controlled by the external temperature was chosen to be the temperature sensors for our model. This was chosen since the operating range we are working with is low i.e. from 25°C to 45°C , hence we linearised the response of the thermistor across the range of operation with another resistor whose value is carefully calibrated, for our case the resistance value was chosen as $6.8\text{k}\Omega$.
- Analog to Digital Converter (ADC) : Since raspberry pi has no analog channels , the temperature values from the thermistor had to be digitised by an ADC and then fed to the raspberry pi.
- PowerSupply : We chose a AC/DC converter whose rating was 5V and 1A to provide the DC current supply to our heater which in turn heated the cup which was placed on it.

C PWM circuit

An off the shelf standalone PWM circuit was designed and tested in LtSpice. The PWM circuit works on a 5V supply and has an output waveform whose voltage ranges between the rails of the output OPAMP , in our case it is between 0V and 5V. As shown in the figure 14, the entire circuit can be broken down into three parts as done in [6] :

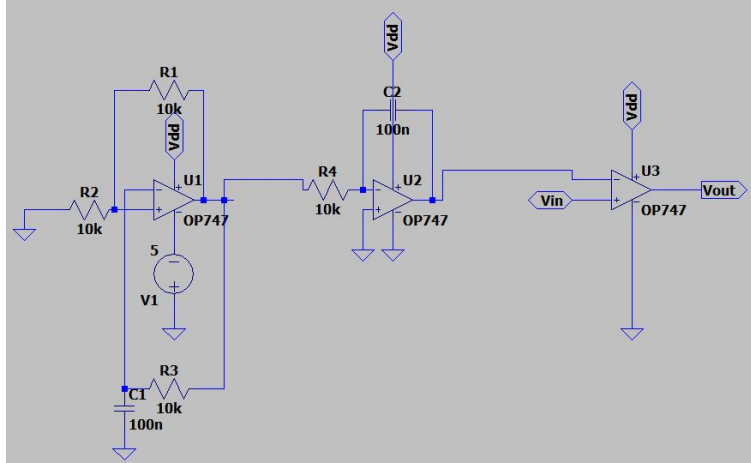


Figure 14: PWM circuit: Detailed scchematic

- Square wave generator : The part of the circuit containing the OPAMP named $U1$, is a positive feedback system called Schmitts trigger to generate an output square waveform whose frequency is defined by $R3$ and $C1$. For our case a frequency of around $500Hz$ is used, since the time constant of the plant is in minutes, anything in seconds or milliseconds will be fast enough to help us heat the system.
- Integrator : The square wave is then integrated upon to generate a triangular waveform with the same frequency and the same voltage range, this functionality is done by the OPAMP $U2$.
- Output Comparator: The reference signal is then compared against this generated traingular waveform with the help of an OPAMP $U3$, used in open loop condition as a comparator to generate the required PWM waveform.

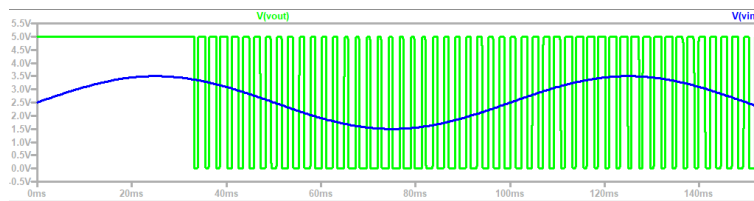


Figure 15: PWM circuit:Output Waveform

A test sinusoid signal of $1Hz$ is used to see the output PWM waveform. There is a latency of around $35ms$, before the postive feedback loop starts to work, beyond which it stabilises and we get the expected PWM waveform. The selected OPAMPS need to be such that the slew rate is much lesser than the frequency of operation and the required voltage levels is in the operation levels of the OPAMP. Since our frequency requirements is less i.e. less than $1kHz$, I have used the most popular OPAMP which is the 747, whose specifications match our requirements.

References

- [1] M G Beker, J F J van den Brand, E Hennes1 and D S Rabeling *Newtonian noise and ambient ground motion for gravitational wave detectors*. Journal of Physics:Conference Series,Volume 363.
- [2] M. Khalid and S. Omatu "A neural network controller for a temperature control system," IEEE Control Systems Magazine, vol. 12, no. 3, pp. 58-64, June 1992, doi: 10.1109/37.165518.
- [3] Guralp CMG40-T datasheet "<https://www.guralp.com/documents/MAN-040-0002.pdf>"
- [4] Trillium 240 datasheet datasheet "https://www.passcal.nmt.edu/webfm_send/220"
- [5] Noise characteristics of thermistors: Measurement methods and results of selected devices,Review of Scientific Instruments 88, 024707 (2017)
- [6] John Caldwell Texas Instruments PWM Circuits : *Analog Pulse Width Modulation*